Article

pubs.acs.org/Biomac

Role of Polymer Architecture on the Activity of Polymer–Protein Conjugates for the Treatment of Accelerated Bone Loss Disorders

Bryan S. Tucker,[†,‡,§] Jon D. Stewart,*[,†] J. Ignacio Aguirre,*[,⊥] L. Shannon Holliday,*[,¶] C. Adrian Figg,[†,‡,§] Jonathan G. Messer,[⊥] and Brent S. Sumerlin*[,†,‡,§]

[†]Department of Chemistry, [‡]George and Josephine Butler Polymer Research Laboratory, and [§]Center for Macromolecular Science and Engineering, University of Florida, Gainesville, Florida 32611, United States

[⊥]Department of Physiological Sciences, College of Veterinary Medicine and [¶]Department of Orthodontics, College of Dentistry, University of Florida, Gainesville, Florida 32610, United States

Supporting Information

ABSTRACT: Polymers of similar molecular weights and chemical constitution but varying in their macromolecular architectures were conjugated to osteoprotegerin (OPG) to determine the effect of polymer topology on protein activity in vitro and in vivo. OPG is a protein that inhibits bone resorption by preventing the formation of mature osteoclasts from the osteoclast precursor cell. Accelerated bone loss disorders, such as osteoporosis, rheumatoid arthritis, and metastatic bone disease, occur as a result of increased osteoclastogenesis, leading to the severe weakening of the bone. OPG has shown promise as a treatment in bone disorders; however, it is rapidly cleared from circulation through rapid liver uptake, and frequent, high doses of the protein are necessary to achieve a therapeutic benefit. We aimed to improve the effectiveness of OPG by creating OPG–polymer bioconjugates, employing reversible addition–fragmentation chain transfer polymerization to create well-defined polymers with branching densities varying from linear, loosely branched to densely branched. Polymers with each of these architectures were conjugated to OPG using a "grafting-to" approach, and the bioconjugates were characterized by sodium dodecyl sulfate polyacrylamide gel electrophoresis. The OPG–polymer bioconjugates showed retention of activity in vitro against osteoclasts, and each bioconjugate was shown to be nontoxic. Preliminary in vivo studies further supported the nontoxic characteristics of the bioconjugates, and measurement of the bone mineral density in rats 7 days post-treatment via peripheral quantitative computed tomography suggested a slight increase in bone mineral density after administration of the loosely branched OPG–polymer bioconjugate.

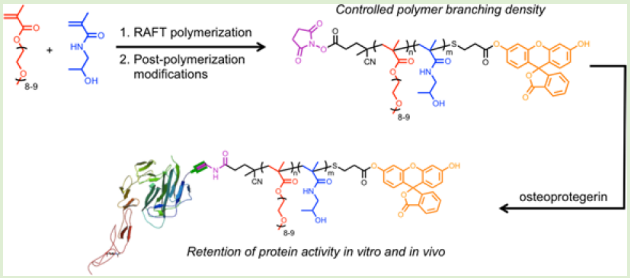

INTRODUCTION

The conjugation of synthetic polymers to proteins has provided a viable route to alter the solubility, activity, and blood circulation times of proteins.[1−8] In particular, attaching poly(ethylene glycol) (PEG) to a protein (i.e., "PEGylation") has proven effective to improve the efficacy of a number of clinically approved therapeutic proteins.[9−13] This increase in therapeutic effectiveness is most often attributed to an increased hydrodynamic diameter of the protein after bioconjugation, thereby decreasing renal filtration and prolonging blood circulation time.[13]

Advances in reversible-deactivation radical polymerization (RDRP) methods have provided a useful toolbox to control the molecular weights, molecular weight distributions, and architectures of polymers used in bioconjugations. Atom transfer radical polymerization (ATRP),[7,14] nitroxide-mediated polymerization (NMP),[15−17] and reversible addition–fragmentation chain transfer (RAFT) polymerization[3,18−23] have all been successfully utilized to immobilize well-defined polymers to a variety of proteins.

Traditionally, polymer–protein bioconjugates are prepared by a "grafting-to" method, which uses a reactive end group on the polymer to react with a specific functional group on the protein, most often primary amines or thiols found in lysine or cysteine residues, respectively.[3,17,24,25,26] This method provides the ability to completely characterize preformed polymers prior to reaction with a protein. The well-defined polymers derived from RDRP techniques have allowed end group control, either by postpolymerization modifications or through the use of a functionalized initiator, leading to well-defined bioconjugates with control over the site-specificity and multiplicity of the polymers.[3,24−29] The versatility of RDRP techniques has also been further demonstrated in a rapidly growing area of bioconjugations using a "grafting-from" strategy, which uses a protein as a macroinitiator or macrochain transfer agent to grow polymers directly from the protein.[2,7,14,30,31,32] The grafting-from method provides some advantages compared to the grafting-to method such as purification (e.g., separation of unreacted monomers vs separation

Received: May 10, 2015
Revised: June 11, 2015

 © XXXX American Chemical Society

DOI: 10.1021/acs.biomac.5b00623
Biomacromolecules XXXX, XXX, XXX−XXX

of unreacted polymers) and control over the number of polymers per protein.

There have been a number of studies that use polymer−peptide bioconjugates to treat degenerative bone diseases and elicit bone growth.[33−35] In the present research, we investigated the effect of conjugating a variety of polymer architectures to osteoprotegerin (OPG), a therapeutically viable protein used in the treatment of osteoporosis and other degenerative bone diseases caused by increased osteoclastic bone resorption.[36−39] OPG is a naturally occurring soluble decoy receptor involved in the regulation of bone resorption by binding to the receptor activator of nuclear factor kappa B (RANK) ligand (L), preventing RANKL from binding to its target receptor, RANK, on the surface of premature osteoclasts.[40−43] By inhibiting the RANK/RANKL interaction, OPG prevents osteoclast differentiation and activation, which reduces bone resorption.[44−49] Treatment of degenerative bone disorders with OPG has been promising, and a recent study indicated that OPG may also be useful in the treatment of muscular dystrophy.[50] However, OPG has a very short in vivo half-life, and multiple doses are required to achieve a therapeutic benefit. Previous studies have shown that conjugating OPG with PEG can improve the blood circulation time of OPG (i.e., the pharmacokinetics), but binding with RANKL (i.e., the pharmacodynamics) was reduced.[51,52] Further studies suggested that changing the architecture of the polymer from linear to branched could provide the increased pharmacokinetics without complete elimination of the pharmacodynamics of the protein.[53]

We sought to further investigate the effect of polymer branching density on the activity of a series of OPG−polymer bioconjugates. Three polymers of varying branching density were synthesized, including linear PEG, loosely branched PEG, and densely branched PEG, while the molecular weight of each architecture was held relatively constant. Each of the unique architectures was then conjugated to OPG via a grafting-to approach using the activated ester, *N*-hydroxysuccinimide (NHS), in the polymer end group. Control over the multiplicity of polymers per protein was elicited by adjusting the pH of the solution to favor functionalization of the *N*-terminus of the protein.[3] Using a grafting-to method allowed complete polymer characterization and end group modifications prior to coupling with a valuable therapeutic protein. The OPG−PEG bioconjugates were analyzed by sodium dodecyl sulfate polyacrylamide gel electrophoresis (SDS-PAGE) to ensure successful conjugation, and the retention of protein activity was demonstrated using an in vitro osteoclast inhibition assay, which showed that each bioconjugate retained high activity against osteoclast formation. Finally, preliminary in vivo studies using peripheral quantitative computed tomography indicated improved bone mineral density of the loosely branched bioconjugate relative to other OPG−polymer architectures.

MATERIALS AND METHODS

Materials. Methacryloyl chloride (Alfa Aesar, 97%), 1-amino-2-propanol (Alfa Aesar, 94%), succinic anhydride (TCI America, >95%), triethylamine (TEA, Alfa Aesar, 99%), hydrazine (Alfa Aesar, 98+%), tris(2-carboxyethyl)phosphine·HCl (TCEP, Alfa Aesar, 98%), methoxypolyethylene glycol (mPEG, Fluka, M_n = 5000 g/mol), 1-ethyl-3-(3-(dimethylamino)propyl)carbodiimide·HCl (EDC·HCl, Sigma-Aldrich, 98%), *N*-hydroxysuccinimide (NHS, Sigma-Aldrich, 99%), trioxane (Acros Organics, 99.5%), dichloromethane (BDH, 99.5%), diethyl ether (Fisher Chemicals), 1,4-dioxane (Fisher Chemicals, 99%), *N*,*N*-dimethylformamide (DMF, EMD, 99.8%), *N*,*N*-dimethylacetamide (DMAc, Sigma-Aldrich, 99%), deuterium oxide (D_2O, Cambridge Isotope, 99.9%), and chloroform-*d* ($CDCl_3$, Cambridge Isotope, 99.8%) were used as received. The 2,2′-azobisisobutronitrile (AIBN, Sigma-Aldrich, 98%) was recrystallized from ethanol. Poly(ethylene glycol)methyl ether methacrylate (PEGMA, Sigma-Aldrich, M_n = 500 g/mol) was passed through a column of basic alumina prior to use. The 4-(cyanopentanoic acid) dithiobenzoate (CDB) and 4-cyano-4-[(dodecylsulfanylthiocarbonyl)sulfanyl]pentanoic acid (CDTPA) were synthesized according to a previously published procedure.[54]

Instrumentation. ^{1}H NMR spectra were recorded on a Varian Innova2 500 MHz or a Varian Mercury 300 MHz NMR spectrometer using the residual solvent signal as a reference. Molecular weight and molecular weight distributions were determined by gel permeation chromatography (GPC) in DMAc with 50 mM LiCl at 50 °C and a flow rate of 1.0 mL min^{-1} (Agilent isocratic pump, degasser, and autosampler; columns, (i) PLgel 5 μm guard + two ViscoGel I-series G3078 mixed bed columns, molecular weight range 0−20 × 10^3 and 0−100 × 10^4 g mol^{-1}; or (ii) PLgel 5 μm guard + two PLgel 5 μm Mixed-D columns, molecular weight range 200−400,000 g mol^{-1}). Detection consisted of (i) Wyatt Optilab T-rEX refractive index detector operating at 658 nm and a Wyatt miniDAWN Treos light scattering detector operating at 659 nm or (ii) Wyatt OptilabDSP interferometric refractometer operating at 690 nm and a Wyatt DAWN EOS light scattering detector operating at 685 nm. Absolute molecular weights and molecular weight distributions were calculated using the Wyatt ASTRA software. UV−vis measurements were obtained using a Varian Carey 500 Scan UV−vis-NIR (near-infrared) spectrophotometer.

Synthesis. *N-(2-hydroxypropyl)methacrylamide (HPMA).* To a three-neck, 2 L round-bottom flask equipped with a mechanical stirring device, thermometer, and addition funnel was added 1-amino-2-propanol (75 mL, 0.96 mol). The reagent was dissolved in dichloromethane (1 L) and cooled to −5 °C in a salt-ice bath. Methacryloyl chloride (46 mL, 0.47 mol) was then added dropwise via addition funnel. The reaction was stirred for 30 min at 0 °C then slowly warmed to room temperature and left to stir overnight. The reaction was filtered to remove 1-amino-2-propanol hydrochloride, and the filtrate was concentrated to 500 mL and placed in a −20 °C freezer overnight to crystallize the product. The resultant HPMA was isolated by filtration and recrystallized from acetone at −20 °C (52 g, 76%). ^{1}H NMR (300 MHz, D_2O) δ: 5.72 (1H, s, CH_2=C), 5.47 (1H, t, CH_2=C), 3.96 (1H, m, $CH_2CH(CH_3)OH$), 3.30 (2H, m, $CH_2CH(CH_3)OH$), 1.95 (3H, s, CH_2=CCH_3), 1.18 (3H, d, $CH_2CH(CH_3)OH$).

Methoxypolyethylene Glycol (mPEG)-Succinic Acid (mPEG-COOH). To a 40 mL scintillation vial with septum cap and stir bar were added mPEG (1.93 g, 0.386 mmol), succinic anhydride (201 mg, 2.01 mmol), and TEA (218 mg, 2.13 mmol). The reagents were dissolved in dry dichloromethane (10 mL) and allowed to stir at room temperature. The reaction was monitored by ^{1}H NMR spectroscopy to observe the appearance of methylene protons adjacent to the forming ester at 4.2 ppm. The reaction was quenched at 4 h, and the polymer was purified by precipitation into diethyl ether (3×, 200 mL).

*mPEG-NHS Ester (**P1**).* To a 20 mL scintillation vial with septum cap and stir bar were added mPEG-COOH (500 mg, 0.1 mmol) and NHS (13 mg, 0.12 mmol). The reagents were dissolved in dry dichloromethane (5 mL) and purged with N_2. EDC·HCl (24 mg, 0.13 mmol) was dissolved in dichloromethane (2 mL) and added to the reaction with stirring. The reaction was allowed to stir at room temperature overnight followed by precipitation into diethyl ether (500 mL). The polymer was filtered and dried under vacuum. The activated ester polymer was used without further purification.

Poly(polyethylene glycol methyl ether methacrylate) (PolyPEGMA$_{11}$). PEGMA (7.86 g, 15.7 mmol), CDB (223 mg, 0.798 mmol), and AIBN (25.6 mg, 0.156 mmol) were added to a 25 mL Schlenk flask with magnetic stir bar. Trioxane (142 mg) was added as an internal reference, and the reagents were dissolved in 1,4-dioxane (9 mL). The flask was sealed with a rubber septum, and the bright red solution was degassed via three freeze−pump−thaw cycles. The mixture was placed in an oil bath at 70 °C with stirring, and the reaction was monitored by GPC and quenched at 2 h. The polymer

DOI: 10.1021/acs.biomac.5b00623
Biomacromolecules XXXX, XXX, XXX−XXX

was purified by dialysis against water using a 3500 MWCO dialysis membrane, and a dark red oil was isolated after lyophilization. The sample was then dissolved in DMF, and hydrazine was used to remove the dithiobenzoate end group ($M_{n,\,GPC}$ = 6040 g/mol, $Đ$ = 1.08).

Fluorescein Conjugation to PolyPEGMA$_{11}$. PolyPEGMA$_{11}$ (163 mg, 2.69 × 10^{-2} mmol) was dissolved in DMF (3 mL) in a 20 mL scintillation vial with septum cap and purged with N_2. TCEP (9.5 mg, 3.3 × 10^{-2} mmol) dissolved in DMF/H_2O (9/1) was added to the reaction, followed by the addition of TEA (4.9 mg, 3.5 × 10^{-2} mmol) and acryloyl(fluorescein) (0.12 mg, 3.1 × 10^{-4} mmol). The reaction was left to stir at room temperature for 16 h, and 1-(2-hydroxyethyl)-1H-pyrrole-2,5-dione (4.9 mg, 3.5 × 10^{-2} mmol) was added as a solution in DMF. The reaction was allowed to stir for 2 h and then dialyzed against water using a 3500 MWCO dialysis membrane. The product was isolated by lyophilization (158 mg).

*NHS Activation of PolyPEGMA$_{11}$-Fluorescein (**P2**).* PolyPEGMA$_{11}$-fluorescein (147 mg, 2.43 × 10^{-2} mmol) and NHS (4.1 mg, 3.6 × 10^{-2} mmol) were dissolved in dry dichloromethane (2 mL). The reaction was purged with N_2, and EDC·HCl (5.5 mg, 2.9 × 10^{-2} mmol) was added as a solution in dichloromethane (0.5 mL). The reaction was left to stir overnight at room temperature. Dichloromethane was removed in vacuo, and the polymer was used without further purification.

Copolymerizations of PEGMA and HPMA. RAFT copolymerizations were performed using CDTPA and AIBN as the CTA and initiator, respectively, with [CTA]:[I] = 5:1. The monomer feed ratios were varied according to Table S1 of the Supporting Information, and the total monomer conversions were limited to ≤16%. The monomers, CTA, initiator, and trioxane were added to a 20 mL scintillation vial equipped with a magnetic stir bar and septum cap, dissolved in DMAc (3 M), purged with N_2 for 30 min, and added to a preheated reaction block at 60 °C. The monomer conversions were determined from ^{1}H NMR spectroscopy by integrating the vinyl protons from each monomer relative to the trioxane standard. The reactivity ratios were calculated graphically using the Finemann−Ross method, where r_1 is given by the slope and r_2 is given by the negative intercept of a plot of G versus H (Tables S1 and S2 and Figure S6, Supporting Information).

Poly(HPMA$_9$-co-PEGMA$_6$). HPMA (1.00. g, 6.98 mmol), PEGMA (1.18 g, 2.36 mmol), CDTPA (92.4 mg, 0.229 mmol), AIBN (8.2 mg, 0.050 mmol), and trioxane (100 mg) as an internal standard were added to a 20 mL scintillation vial equipped with a septum cap and magnetic stir bar. The reagents were dissolved in DMAc (3 mL), purged with N_2 for 30 min, and added to a preheated heating block at 60 °C. The reaction was quenched after 4 h by exposing the contents to oxygen, and the polymer was purified by dialysis against water using a 3500 MWCO membrane and lyophilized to yield an amorphous solid ($M_{n,\,GPC}$ = 7020 g/mol, $Đ$ = 1.07).

Poly(HPMA$_9$-co-PEGMA$_6$)-Fluorescein. Poly(HPMA$_9$-*co*-PEGMA$_6$) (150 mg, 2.0 × 10^{-2} mmol) was dissolved in DMF (3 mL) with stirring in a 20 mL scintillation vial with septum cap. Hydrazine (0.05 mL, 2 mmol) was added, and the reaction turned colorless immediately. After 30 min, the mixture was placed in a 3500 MWCO dialysis membrane and dialyzed against water followed by lyophilization to isolate the polymer. The end-group removed Poly(HPMA$_9$-*co*-PEGMA$_6$) (118 mg, 1.68 × 10^{-2} mmol) was dissolved in DMF (3 mL) in a 20 mL scintillation vial with septum cap and stir bar and purged with N_2 for 30 min. TCEP (5.6 mg, 2.0 × 10^{-2} mmol) was then added as a solution in water (0.5 mL), followed by TEA (2.64 mg, 2.61 × 10^{-2} mmol). Acryloyl(fluorescein) (0.1 mg, 2 × 10^{-4} mmol) was added, and the reaction was allowed to stir at room temperature for 20 h. 1-(2-hydroxyethyl)-1H-pyrrole-2,5-dione (3.2 mg, 2.3 × 10^{-2} mmol) in DMF (0.5 mL) was added and stirred 2 h, and the mixture was dialyzed against water using a 3500 MWCO dialysis membrane. The product was isolated by lyophilization to give a yellow solid (100 mg).

*NHS Activation of Poly(HPMA$_9$-co-PEGMA$_6$)-Fluorescein (**P3**).* Poly(HPMA$_9$-*co*-PEGMA$_6$)-fluorescein (89.1 mg, 1.27 × 10^{-2} mmol) and NHS (1.8 mg, 1.6 × 10^{-2} mmol) were dissolved in dry dichloromethane (2 mL). The reaction was briefly purged with N_2, and EDC·HCl (3.0 mg, 1.6 × 10^{-2} mmol) was added as a solution in dichloromethane (0.5 mL). The reaction was left to stir overnight at room temperature. Dichloromethane was removed in vacuo, and the polymer was used without further purification.

Conjugation to OPG. Two vials of recombinant human TNFRSF 11B-487 (OPG, 1 mg protein, Creative Biomart, His-tagged, lot #265155) were warmed to room temperature, and each was dissolved in phosphate buffer (250 μL, 100 mM, pH 7.5). Both solutions were combined and placed in a Millipore Amicon Ultra 0.5 10 000 Da MWCO ultrafiltration unit and centrifuged at 14 000 rpm at room temperature for 10 min to remove interfering excipients. The protein solution was diluted with phosphate buffer (500 μL, 100 mM, pH 7.5) and centrifuged as before. This process was repeated three more times to desalt the OPG prior to conjugation. The final OPG solution (*ca.* 90 μL) had a concentration of approximately 22 μg/mL and was stored on ice.

Activated polymers were dissolved in phosphate buffer (100 mM, pH 7.5) at concentrations of 2.5 mM immediately prior to conjugation. OPG conjugations were carried out in 50 μL total volumes by mixing OPG stock (20 μL, 7.3 nmol), polymer stock (15 μL, 37 nmol), and phosphate buffer (15 μL, 100 mM, pH 7.5). After incubating for 24 h at room temperature, each reaction mixture was placed in a separate Millipore Amicon Ultra 0.5 10 000 Da MWCO ultrafiltration unit, diluted with phosphate buffer (450 μL, 100 mM, pH 7.5), and centrifuged at 14 000 rpm for 10 min at room temperature. This washing was repeated three additional times. The final concentrated protein samples were stored at 4 °C prior to biological assays.

Mouse Marrow Culture. The 1,25-dihydroxyvitamin D_3 (1,25D_3)-stimulated mouse marrow, in which osteoblasts and osteoclasts differentiate coordinately over a period of 6 days, was produced as described previously.[55] Femora and tibia from Swiss-Webster mice (8−20 g) that had been killed by cervical dislocation were dissected from adherent tissue, and marrow was removed by clipping both bone ends, inserting a syringe with a 25 gauge needle, and flushing the marrow using αMEM plus 10% fetal bovine serum (αMEM D10). The marrow was washed twice with αMEM D10 and then plated at a density of 1 × 10^6 cells/cm^2 on tissue culture plates for 6 days in αMEM D10 plus 10^{-8} M 1,25D_3. Cultures were fed on day 4 by replacing half the media per plate and adding fresh 1,25D_3. OPG and OPG conjugates were added on day 1 and refreshed on day 4. After 6 days in culture, osteoclasts were abundant in control cultures. Cells were fixed with 2% paraformaldehyde in citrate buffer for 20 min, permeabilized by treatment with 1% Triton X-100 for 10 min, washed in citrate buffer, and osteoclasts were detected by staining for tartrate-resistant acid phosphatase (TRAcP) activity, which is a specific marker for mouse osteoclasts, using the Leukocyte Acid Phosphatase (TRAP) kit from Sigma (St Louis, MO). Cells expressing TRAcP activity were documented as described previously.[55] The University of Florida Institutional Animal Care and Usage Committee approved this protocol.

Cell Cytotoxicity Assay. RAW 264.7 cells were grown as described previously.[56] Raw 264.7 cells (ATCC) were plated at a density of 1.25 × 10^4 cells per well in 24-well plates and treated with OPG or derivatives of OPG as indicated. Adherent cells from three random fields per well (250 μm^2) were counted and then averaged for each well. Live cells were counted on day 2. On day 4, the cells were fixed with 2% formaldehyde prior to counting. No overt signs of toxicity, excess nonadherent cells, or cell debris were noted on either days 2 or 4.

Animals and Experimental Groups. A total of 20 jugular vein-cannulated male Sprague−Dawley rats aged 8−10 weeks arrived to the Animal Care Services, University of Florida from a commercial vendor (Charles River, Ltd.). After arrival, rats were housed individually in ventilated cages. The housing room was maintained at 68−79 °F with an average humidity of 30−70% and a 12:12 h light/dark cycle. All animal procedures were approved by the Institutional Animal Care and Use Committee at the University of Florida (Gainesville, FL).

After a week of acclimation, rats were randomized into the following five experimental groups (n = 4):

(1) Group of rats euthanized at the beginning of the experiment and received no treatment (**Baseline control**).

DOI: 10.1021/acs.biomac.5b00623
Biomacromolecules XXXX, XXX, XXX−XXX

(2) Group of rats that received a single bolus intravenous (IV) injection of OPG alone (0.4 mg/kg) diluted in phosphate buffer (pH 7.2) (**Unmodified OPG**).
(3) Group of rats that received a single bolus IV injection of the linear PEG−OPG bioconjugate (0.4 mg/kg) diluted in phosphate buffer (pH 7.2) (**OPG1**).
(4) Group of rats that received a single bolus IV injection of the densely branched PEG−OPG bioconjugate (0.4 mg/kg) diluted in phosphate buffer (pH 7.2) (**OPG2**).
(5) Group of rats that received a single bolus IV injection of the loosely branched PEG−OPG bioconjugate (0.4 mg/kg) diluted in phosphate buffer (pH 7.2) (**OPG3**). Only one of the four assigned rats was injected in this group due to loss of the bioconjugate sample during filtration.

Rats from the baseline group and those rats after completion of the 7-day period were euthanized by CO_2 inhalation followed by thoracotomy. Left femurs were excised and stripped of musculature, placed in 10% buffered formalin for 48 h, and transferred to 70% ethanol.

Peripheral Quantitative Computed Tomography (pQCT). For the pQCT analysis, left femurs from all rats were scanned using a Stratec XCT Research M instrument (Norland Medical Systems; Fort Atkinson, WI) with software version 5.40. Scans were performed at distances of 2, 4, and 6 mm proximal to the distal femur epiphyseal growth plate. At this location, corresponding to the primary and secondary spongiosa, is where endochondral ossification takes place and bone grows in length and undergoes remodeling. Trabecular (trab) bone mineral content (BMC), trab bone mineral density (trab BMD) and trab bone area (trab BA) were determined as previously described.[57]

RESULTS AND DISCUSSION

Polymer Synthesis. Linear PEG, **P1**, was synthesized by modifying the end group of commercially available mPEG (M_n = 5000 g/mol) to contain an NHS activated ester (Scheme 1),

Scheme 1. Ring Opening of Succinic Anhydride with mPEG and Formation of an NHS Activated Ester To Give P1

rendering the linear polymer reactive toward amine residues in the protein.

The densely branched PEG architecture, **P2** (polyPEGMA$_{11}$), was synthesized using RAFT polymerization of PEGMA (Scheme 2; Figure S3, Supporting Information). Because we aimed to study the effect of varying branching density on conjugate activity, the molecular weight of the polymers was held constant, targeting an M_n of 5000 g/mol. Reports have suggested in vivo cytotoxicity of dithiobenzoate end groups;[58] therefore, the RAFT group was removed by aminolysis. The resultant thiol, a useful handle for further functionalization,[59] was exploited using Michael addition to incorporate fluorescein as a convenient marker for in vitro and in vivo monitoring. The end group removal and fluorescein conjugations were confirmed by UV−vis spectroscopy (Figure S4, Supporting Information), and the carboxylic acid α-end group was then converted to an NHS ester for bioconjugations.

The loosely branched PEG architecture, **P3** (poly(HPMA$_9$-*co*-PEGMA$_6$), was prepared by copolymerizing PEGMA with HPMA via RAFT polymerization (Scheme 3; Figure S5, Supporting Information). We first studied the copolymerization kinetics of PEGMA and HPMA by determining the monomer reactivity ratios. The Finemann−Ross method was used to calculate r_1 (monomer reactivity ratio for PEGMA) = 0.98 and r_2 (monomer reactivity ratio for HPMA) = 0.52 (Tables S1 and S2, Figure S6, Supporting Information). These values indicate that the copolymerization of the monomers is not random, with PEGMA being preferentially consumed during the reaction. Therefore, we altered the monomer feed ratio to target approximately 50% of the number of PEGMA repeat units as that of the densely branched polymer described previously. While the polymer likely contains a gradient microstructure rather than a random copolymer, we believe that the polymer contains the lower branching density needed to study the effect of branching density on protein activity. The RAFT group was removed by aminolysis, fluorescein was conjugated through Michael addition (Figure S7, Supporting Information), and the carboxylic acid end group was converted to an NHS ester.

Protein Conjugations. OPG was modified with each of the polymer architectures using a grafting-to approach, in which the pH value of the reaction was controlled to increase the probability of selectively deprotonating the amine-terminus of the protein, while the primary amines of lysine residues were expected to be protonated and therefore rendered less nucleophilic (Scheme 4).[60,61] Since coupling reactions of macromolecular reagents can be less efficient than those of small molecules, five molar equivalents of polymer were used for each bioconjugation. A control experiment was also performed, in which pure OPG in the absence of polymer was subjected to the same reaction and purification conditions employed during the bioconjugation reaction and work-up. The purified OPG−PEG conjugates (**OPG1**, **OPG2**, and **OPG3** for the linear PEG, densely branched PEG, and loosely branched PEG architectures, respectively) were analyzed by SDS-PAGE, which demonstrated successful polymer conjugation to OPG in addition to some remaining unmodified protein (Figure 1).

In Vitro Osteoclast Inhibition Assay. The in vitro activity of each bioconjugate was measured using an osteoclast inhibition assay with 1,25-dihydroxyvitamin D_3-stimulated mouse marrow cells and bioconjugate concentrations of 2, 20, and 200 ng/mL administered on days 1 and 4. Cells were fixed at day 6 and stained for TRAcP, a marker for osteoclast activity.[62] Cells were divided into mononuclear, multinuclear (2−10 nuclei), and giant (>10 nuclei), with each cell population representing increasingly mature osteoclast cells. The osteoclast levels were counted, and the results indicated that while 2 ng/mL was too dilute to inhibit osteoclast growth for the unmodified OPG or **OPG1** and **OPG2**, the osteoclast count was reduced for **OPG3**. Furthermore, a concentration of 20 ng/mL resulted in decreased osteoclast counts for all samples receiving OPG relative to the control (no OPG). At a concentration of 200 ng/mL, osteoclasts were completely inhibited for all of the conjugates (Figure 2). Importantly, each bioconjugate of OPG retained antiosteoclast activity at concentrations of 20 and 200 ng/mL. To provide evidence that the decrease in osteoclast activity is due to the inhibition of osteoclast maturation by the OPG−RANKL interaction and not due to general cytotoxicity of the bioconjugates, a cell cytotoxicity study was performed using cells that serve as a model for macrophages (Figure 3). The cells were shown to have near-quantitative viability at 2 and 4 days at the concentrations used in the osteoclast inhibition assay described, which suggested that each bioconjugate was nontoxic and supported the observation that the decrease in osteoclast maturation was indeed a result of OPG−RANKL binding.

Conjugation of even a single polymer can greatly reduce the activity of many proteins.[6,63−66] Thus, these results were

DOI: 10.1021/acs.biomac.5b00623
Biomacromolecules XXXX, XXX, XXX−XXX

Scheme 2. (A) RAFT Polymerization of PEGMA To Afford a Densely Branched Polymer, PolyPEGMA$_{11}$, Followed by Aminolysis To Remove the RAFT Group. (B) Michael Addition Using Acryloyl(fluorescein). (C) Formation of the NHS Activated Ester To Give P2

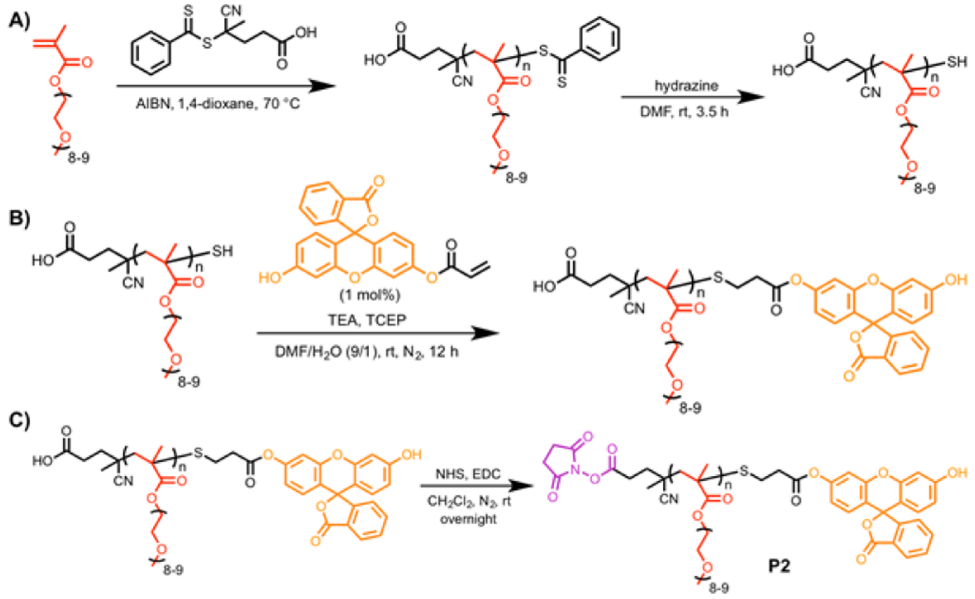

Scheme 3. (A) RAFT Copolymerization of PEGMA and HPMA. (B) RAFT Group Removal and Michael Addition with Acryloyl(fluorescein). (C) Formation of NHS Ester To Afford P3

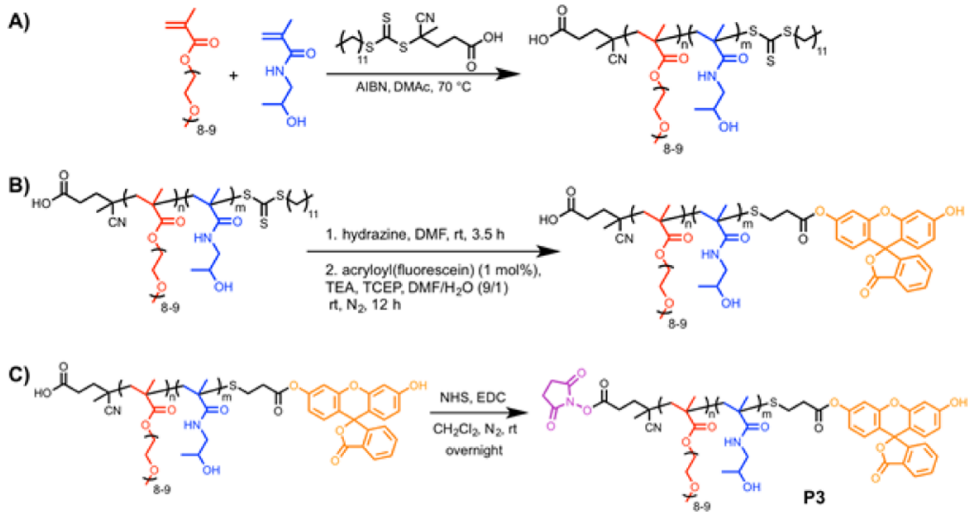

Scheme 4. OPG Bioconjugations with (A) P1 To Form OPG1, (B) P2 To Form OPG2, and (C) P3 To Form OPG3. Protein Structure from the PDB (3URF)

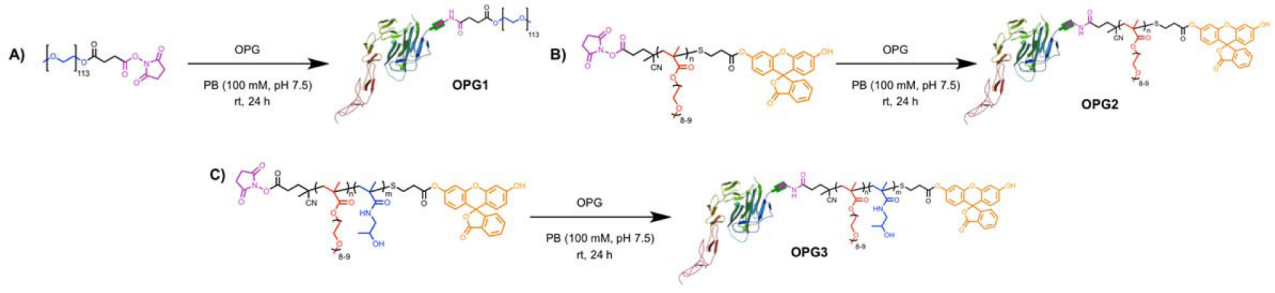

promising because the OPG bioconjugates retained their ability to prevent osteoclast formation, which suggests that they may also decrease bone resorption in vivo. Furthermore, the loosely branched bioconjugate, **OPG3**, actually had higher in vitro activity than either **OPG1** or **OPG2**, as indicated in a lower osteoclast count (Figure 2).

DOI: 10.1021/acs.biomac.5b00623
Biomacromolecules XXXX, XXX, XXX−XXX

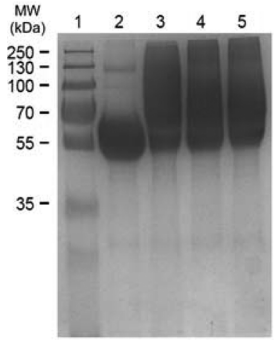

Figure 1. SDS-PAGE analysis of OPG bioconjugates. Lane: (1) molecular weight marker, (2) unmodified OPG, (3) **OPG1**, (4) **OPG3**, and (5) **OPG2**.

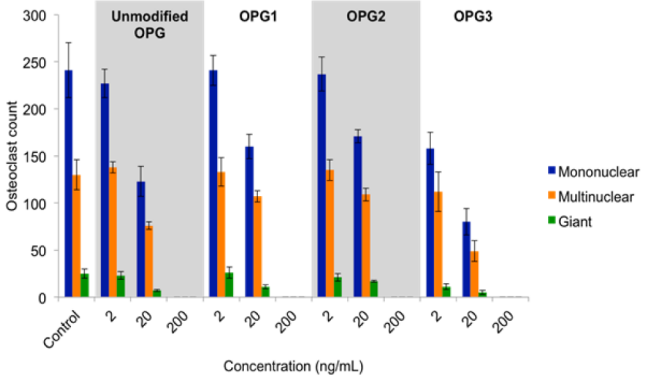

Figure 2. Osteoclast inhibition assay using 1,25-dihydroxyvitamin D_3-stimulated mouse marrow cells. The control is the osteoclast count of untreated cells. Background shading indicates different OPG samples with doses on days 1 and 4, each with three concentrations of 2, 20, and 200 ng/mL. Three cell types were counted—mononuclear, multinuclear, and giant—indicated by the different bar colors blue, orange, and green, respectively.

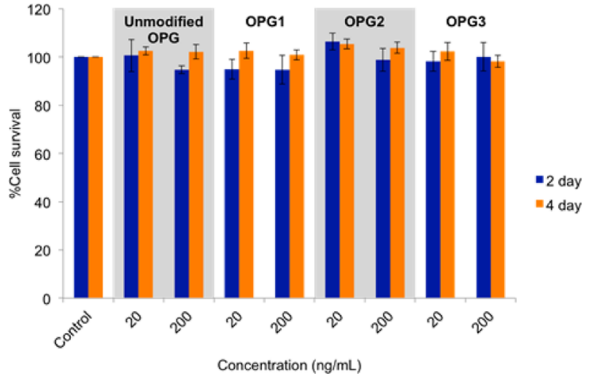

Figure 3. Cell cytotoxicity assay using RAW 264.7 cells shown as the percentage of cell survival relative to a control, which was untreated cells. Each bioconjugate, indicated by background shading, was administered at concentrations of 20 and 200 ng/mL, and live cells were counted at 2 d (blue) and fixed with formaldehyde and counted at 4 d (orange). Each sample is the average of four replicates.

In Vivo Skeletal Effect Study. We aimed to show that the effects of osteoclast inhibition observed in vitro could also be translated to in vivo effectiveness. Since OPG ultimately prevents differentiation and activation of osteoclasts, we reasoned that we could monitor the efficacy of our bioconjugates in vivo by monitoring the bone mass and bone volume in rats. A facile and reliable way to determine bone mass is by determining bone mineral density (BMD), a surrogate of bone mass, using pQCT. We tested the antiresorptive activity of each bioconjugate in vivo by measuring trabecular (trab) BMD, trabecular bone mineral content (trab BMC), and trabecular bone area (trab BA) at the distal femoral metaphyses of Sprague–Dawley rats at different distances from the growth plate. For this purpose, 20 cannulated rats were divided into five groups. One group was sacrificed at the beginning of the experiment and received no treatment to serve as a baseline control. The other four groups received single bolus intravenous injections of unmodified OPG, **OPG1**, **OPG2**, or **OPG3** and were euthanized 7 days post-treatment. Femurs were collected post-mortem, and BMD was analyzed by pQCT at distances of 2, 4, and 6 mm proximal to the distal epiphyseal growth plate (Figure S8, Supporting Information).

The pQCT analyses showed increased femur trab BMD, trab BMC, and trab BA at the distal metaphysis of rats treated with **OPG3** compared to rats from the baseline, unmodified OPG, **OPG1**, and **OPG2** groups (Figure 4; Figure S9, Supporting Information). While the linear and densely branched protein bioconjugates showed no increase in BMD from either unmodified OPG or the baseline control, we believe that the loosely branched bioconjugate has enhanced antiresorptive activity, consistent with the in vitro data described above. Furthermore, since even unmodified OPG had no significant

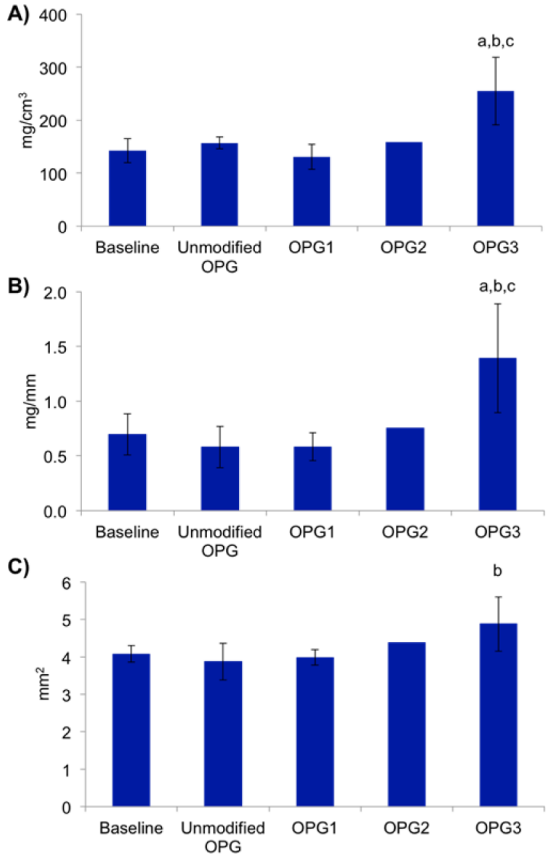

Figure 4. (A) Bone mineral density, (B) bone mineral content, and (C) bone mineral area of OPG bioconjugates as the average from 2–6 mm from the growth plate. Statistical analysis was accomplished with one-way analysis of variance (ANOVA) followed by post-ANOVA: multiple comparison Tukey Test or nonparametric Kruskal–Wallis test; a = different from baseline, b = different from unmodified OPG, and c = different from OPG1.

DOI: 10.1021/acs.biomac.5b00623
Biomacromolecules XXXX, XXX, XXX–XXX

bone effect as compared to the control, it is possible that higher concentrations or multiple doses of the bioconjugate would further enhance the bone growth profile. When combined with the nontoxic characteristics shown in the in vitro studies, these in vivo results indicate promise for these materials as an effective therapy in bone degenerative disorders. Further pharmacokinetic studies are necessary to show the enhanced blood circulation half-life of the bioconjugates, but the increase in BMD is an exciting preliminary result that gives hope to the translation from in vitro to in vivo efficacy.

CONCLUSIONS

In summary, three polymers with linear, loosely branched, and densely branched architectures were conjugated to OPG using a grafting-to strategy. Control over the polymer branching density was elicited using RAFT copolymerization of a PEGMA macromonomer with HPMA, a water-soluble monomer that leads to vinyl polymers with good biocompatibility.[67] End group control allowed further functionalization to render the polymers reactive toward primary amines on proteins. Importantly, each bioconjugate was shown to be nontoxic and retained high activity toward the inhibition of osteoclasts. Preliminary in vivo studies further supported the nontoxic character of the OPG bioconjugates, and initial results suggested an increase in the bone mineral density of the loosely branched OPG bioconjugate. A more robust pharmacokinetics study is needed to unequivocally show the therapeutic benefit of OPG−polymer bioconjugates, but this report demonstrates the feasibility of using such a system to treat bone degenerative diseases.

ASSOCIATED CONTENT

Supporting Information

Experimental procedures, GPC chromatograms, ^{1}H NMR spectra, UV−vis spectra, and bone mineral density data. The Supporting Information is available free of charge on the ACS Publications website at DOI: 10.1021/acs.biomac.5b00623.

AUTHOR INFORMATION

Corresponding Author

*E-mail: sumerlin@chem.ufl.edu.
*E-mail: jds2@chem.ufl.edu.
*E-mail: aguirrej@ufl.edu.
*E-mail: SHOLLIDAY@dental.ufl.edu.

Author Contributions

The manuscript was written through contributions of all authors.

Funding

The authors would like to acknowledge the University of Florida Research Foundation and the UF Seed Opportunity Fund for partial support of this work.

Notes

The authors declare no competing financial interest.

REFERENCES

(1) Broyer, R. M.; Grover, G. N.; Maynard, H. D. *Chem. Commun.* **2011**, *47*, 2212−2226.
(2) Sumerlin, B. S. *ACS Macro Lett.* **2012**, *1*, 141−145.
(3) Li, M.; De, P.; Li, H.; Sumerlin, B. S. *Polym. Chem.* **2010**, *1*, 854−859.
(4) Li, H.; Bapat, A. P.; Li, M.; Sumerlin, B. S. *Polym. Chem.* **2011**, *2*, 323−327.
(5) Ryan, S. M.; Frías, J. M.; Wang, X.; Sayers, C. T.; Haddleton, D. M.; Brayden, D. J. *J. Controlled Release* **2011**, *149*, 126−132.
(6) Tao, L.; Liu, J.; Xu, J.; Davis, T. P. *Org. Biomol. Chem.* **2009**, *7*, 3481−3485.
(7) Lele, B. S.; Murata, H.; Matyjaszewski, K.; Russell, A. J. *Biomacromolecules* **2005**, *6*, 3380−3387.
(8) Duncan, R. *Nat. Rev. Cancer* **2006**, *6*, 688−701.
(9) Harris, J. M.; Chess, R. B. *Nat. Rev. Drug Discovery* **2003**, *2*, 214−221.
(10) Veronese, F. M.; Harris, J. M. *Adv. Drug Delivery Rev.* **2002**, *54*, 453−456.
(11) Rajender Reddy, K.; Modi, M. W.; Pedder, S. *Adv. Drug Delivery Rev.* **2002**, *54*, 571−586.
(12) Abuchowski, A.; McCoy, J. R.; Palczuk, N. C.; van Es, T.; Davis, F. F. *J. Biol. Chem.* **1977**, *252*, 3582−3586.
(13) Caliceti, P.; Veronese, F. M. *Adv. Drug Delivery Rev.* **2003**, *55*, 1261−1277.
(14) Averick, S.; Simakova, A.; Park, S.; Konkolewicz, D.; Magenau, A. J. D.; Mehl, R. A.; Matyjaszewski, K. *ACS Macro Lett.* **2012**, *1*, 6−10.
(15) Nicolas, J.; Guillaneuf, Y.; Lefay, C.; Bertin, D.; Gigmes, D.; Charleux, B. *Prog. Polym. Sci.* **2013**, *38*, 63−235.
(16) Becker, M. L.; Liu, J.; Wooley, K. L. *Chem. Commun.* **2002**, 180−181.
(17) Chenal, M.; Boursier, C.; Guillaneuf, Y.; Taverna, M.; Couvreur, P.; Nicolas, J. *Polym. Chem.* **2011**, *2*, 1523−1530.
(18) Li, H.; Li, M.; Yu, X.; Bapat, A. P.; Sumerlin, B. S. *Polym. Chem.* **2011**, *2*, 1531−1535.
(19) Liu, J.; Bulmus, V.; Herlambang, D. L.; Barner-Kowollik, C.; Stenzel, M. H.; Davis, T. P. *Angew. Chem., Int. Ed.* **2007**, *46*, 3099−3103.
(20) Boyer, C.; Bulmus, V.; Liu, J.; Davis, T. P.; Stenzel, M. H.; Barner-Kowollik, C. *J. Am. Chem. Soc.* **2007**, *129*, 7145−7154.
(21) Li, M.; De, P.; Gondi, S. R.; Sumerlin, B. S. *Macromol. Rapid Commun.* **2008**, *29*, 1172−1176.
(22) Cobo, I.; Li, M.; Sumerlin, B. S.; Perrier, S. *Nat. Mater.* **2015**, *14*, 143−159.
(23) Falatach, R.; McGlone, C.; Al-Abdul-Wahid, M. S.; Averick, S.; Page, R. C.; Berberich, J. A.; Konkolewicz, D. *Chem. Commun.* **2015**, *51*, 5343−5346.
(24) Sayers, C. T.; Mantovani, G.; Ryan, S. M.; Randev, R. K.; Keiper, O.; Leszczyszyn, O. I.; Blindauer, C.; Brayden, D. J.; Haddleton, D. M. *Soft Matter* **2009**, *5*, 3038−3046.
(25) Jones, M. W.; Strickland, R. A.; Schumacher, F. F.; Caddick, S.; Baker, J. R.; Gibson, M. I.; Haddleton, D. M. *J. Am. Chem. Soc.* **2012**, *134*, 1847−1852.
(26) Pokorski, J. K.; Hovlid, M. L.; Finn, M. G. *ChemBioChem* **2011**, *12*, 2441−2447.
(27) Nguyen, T. H.; Kim, S.-H.; Decker, C. G.; Wong, D. Y.; Loo, J. A.; Maynard, H. D. *Nat. Chem.* **2013**, *5*, 221−227.
(28) Grover, G. N.; Lee, J.; Matsumoto, N. M.; Maynard, H. D. *Macromolecules* **2012**, *45*, 4958−4965.
(29) Bays, E.; Tao, L.; Chang, C.-W.; Maynard, H. D. *Biomacromolecules* **2009**, *10*, 1777−1781.
(30) Murata, H.; Cummings, C. S.; Koepsel, R. R.; Russell, A. J. *Biomacromolecules* **2013**, *14*, 1919−1926.
(31) Wallat, J. D.; Rose, K. A.; Pokorski, J. K. *Polym. Chem.* **2014**, *5*, 1545−1558.
(32) Pokorski, J. K.; Breitenkamp, K.; Liepold, L. O.; Qazi, S.; Finn, M. G. *J. Am. Chem. Soc.* **2011**, *133*, 9242−9245.
(33) Policastro, G. M.; Lin, F.; Smith Callahan, L. A.; Esterle, A.; Graham, M.; Sloan Stakleff, K.; Becker, M. L. *Biomacromolecules* **2015**, *16*, 1358−1371.
(34) Tang, W.; Ma, Y.; Xie, S.; Guo, K.; Katzenmeyer, B.; Wesdemiotis, C.; Becker, M. L. *Biomacromolecules* **2013**, *14*, 3304−3313.
(35) Moore, N. M.; Lin, N. J.; Gallant, N. D.; Becker, M. L. *Biomaterials* **2010**, *31*, 1604−1611.
(36) Yamaguchi, K.; Kinosaki, M.; Goto, M.; Kobayashi, F.; Tsuda, E.; Morinaga, T.; Higashio, K. *J. Biol. Chem.* **1998**, *273*, 5117−5123.

DOI: 10.1021/acs.biomac.5b00623
Biomacromolecules XXXX, XXX, XXX−XXX

(37) Boyle, W. J.; Simonet, W. S.; Lacey, D. L. *Nature* **2003**, *423*, 337−342.
(38) Simonet, W. S.; Lacey, D. L.; Dunstan, C. R.; Kelley, M.; Chang, M. S.; Lüthy, R.; Nguyen, H. Q.; Wooden, S.; Bennett, L.; Boone, T.; Shimamoto, G.; DeRose, M.; Elliott, R.; Colombero, A.; Tan, H. L.; Trail, G.; Sullivan, J.; Davy, E.; Bucay, N.; Renshaw-Gegg, L.; Hughes, T. M.; Hill, D.; Pattison, W.; Campbell, P.; Sander, S.; Van, G.; Tarpley, J.; Derby, P.; Lee, R.; Boyle, W. J. *Cell* **1997**, *89*, 309−319.
(39) Lacey, D. L.; Timms, E.; Tan, H. L.; Kelley, M. J.; Dunstan, C. R.; Burgess, T.; Elliot, R.; Colombero, A.; Elliot, G.; Scully, S.; Hsu, H.; Sullivan, J.; Hawkins, N.; Davy, E.; Capparelli, C.; Elie, A.; Qian, Y. X.; Kaufman, S.; Sarosi, I.; Shalhoub, V.; Senaldi, G.; Guo, J.; Delaney, J.; Boyle, W. J. *Cell* **1998**, *93*, 165−176.
(40) Luan, X.; Lu, Q.; Jiang, Y.; Zhang, S.; Wang, Q.; Yuan, H.; Zhao, W.; Wang, J.; Wang, X. *J. Immunol.* **2012**, *189*, 245−252.
(41) Yasuda, H.; Shima, N.; Nakagawa, N.; Yamaguchi, K.; Kinosaki, M.; Mochizuki, S.-I.; Tomoyasu, A.; Yano, K.; Goto, M.; Murakami, A.; Tsuda, E.; Morinaga, T.; Higashio, K.; Udagawa, N.; Takahashi, N.; Suda, T. *Proc. Natl. Acad. Sci. U. S. A.* **1998**, *95*, 3597−3602.
(42) Hofbauer, L. C. *Eur. J. Endocrinol.* **1999**, *141*, 195−210.
(43) Hsu, H.; Lacey, D. L.; Dunstan, C. R.; Solovyev, I.; Colombero, A.; Timms, E.; Tan, H. L.; Elliott, G.; Kelley, M. J.; Sarosi, I.; Wang, L.; Xia, X. Z.; Elliott, R.; Chiu, L.; Black, T.; Scully, S.; Capparelli, C.; Morony, S.; Shimamoto, G.; Bass, M. B.; Boyle, W. J. *Proc. Natl. Acad. Sci. U. S. A.* **1999**, *96*, 3540−3545.
(44) Ominsky, M. S.; Li, X.; Asuncion, F. J.; Barrero, M.; Warmington, K. S.; Dwyer, D.; Stolina, M.; Geng, Z.; Grisanti, M.; Tan, H. L.; Corbin, T.; McCabe, J.; Simonet, W. S.; Ke, H. Z.; Kostenuik, P. J. *J. Bone Miner. Res.* **2008**, *23*, 672−682.
(45) Ominsky, M. S.; Stolina, M.; Li, X.; Corbin, T. J.; Asuncion, F. J.; Barrero, M.; Niu, Q.-T.; Dwyer, D.; Adamu, S.; Warmington, K. S.; Grisanti, M.; Tan, H. L.; Ke, H. Z.; Simonet, W. S.; Kostenuik, P. J. *J. Bone Miner. Res.* **2009**, *24*, 1234−1246.
(46) Morony, S.; Capparelli, C.; Sarosi, I.; Lacey, D. L.; Dunstan, C. R.; Kostenuik, P. J. *Cancer Res.* **2001**, *61*, 4432−4436.
(47) Bekker, P. J.; Holloway, D.; Nakanishi, A.; Arrighi, M.; Leese, P. T.; Dunstan, C. R. *J. Bone Miner. Res.* **2001**, *16*, 348−360.
(48) Body, J. J. *Clin. Cancer Res.* **2006**, *12*, 1221−1228.
(49) Bucay, N.; Sarosi, I.; Dunstan, C. R.; Morony, S.; Tarpley, J.; Capparelli, C.; Scully, S.; Tan, H. L.; Xu, W.; Lacey, D. L.; Boyle, W. J.; Simonet, W. S. *Genes Dev.* **1998**, *12*, 1260−1268.
(50) Dufresne, S. S.; Dumont, N. A.; Bouchard, P.; Lavergne, E.; Penninger, J. M.; Frenette, J. *Am. J. Pathol.* **2015**, *185*, 920−926.
(51) Saito-Yabe, M.; Kasuya, Y.; Yoshigae, Y.; Yamamura, N.; Suzuki, Y.; Fukuda, N.; Honma, M.; Yano, K.; Mochizuki, S.-I.; Okada, F.; Okada, A.; Nagayama, Y.; Tsuda, E.; Fischer, T.; Höpner, U.; Zaja, S.; Mueller, J.; Okada, J.; Kurihara, A.; Ikeda, T.; Okazaki, O. *J. Pharm. Pharmacol.* **2010**, *62*, 985−994.
(52) Miyaji, Y.; Kurihara, A.; Kamiyama, E.; Shiiki, T.; Kawai, K.; Okazaki, O. *Xenobiotica* **2009**, *39*, 113−124.
(53) Miyaji, Y.; Kasuya, Y.; Furuta, Y.; Kurihara, A.; Takahashi, M.; Ogawara, K.-I.; Izumi, T.; Okazaki, O.; Higaki, K. *Pharm. Res.* **2012**, *29*, 3143−3155.
(54) Moad, G.; Chong, Y. K.; Postma, A.; Rizzardo, E.; Thang, S. H. *Polymer* **2005**, *46*, 8458−8468.
(55) Ostrov, D. A.; Magis, A. T.; Wronski, T. J.; Chan, E. K. L.; Toro, E. J.; Donatelli, R. E.; Sajek, K.; Haroun, I. N.; Nagib, M. I.; Piedrahita, A.; Harris, A.; Holliday, L. S. *J. Med. Chem.* **2009**, *52*, 5144−5151.
(56) Toro, E. J.; Zuo, J.; Ostrov, D. A.; Catalfamo, D.; Bradaschia-Correa, V.; Arana-Chavez, V.; Caridad, A. R.; Neubert, J. K.; Wronski, T. J.; Wallet, S. M.; Holliday, L. S. *J. Biol. Chem.* **2012**, *287*, 17894−17904.
(57) Ke, H. Z.; Qi, H.; Chidsey-Frink, K. L.; Crawford, D. T.; Thompson, D. D. *J. Bone Miner. Res.* **2001**, *16*, 765−773.
(58) Pissuwan, D.; Boyer, C.; Gunasekaran, K.; Davis, T. P.; Bulmus, V. *Biomacromolecules* **2010**, *11*, 412−420.
(59) Roth, P. J.; Boyer, C.; Lowe, A. B.; Davis, T. P. *Macromol. Rapid Commun.* **2011**, *32*, 1123−1143.
(60) Klok, H.-A. *J. Polym. Sci., Part A: Polym. Chem.* **2005**, *43*, 1−17.
(61) Sélo, I.; Négroni, L.; Créminon, C.; Grassi, J.; Wal, J. M. *J. Immunol. Methods* **1996**, *199*, 127−138.
(62) Minkin, C. *Calcif. Tissue Int.* **1982**, *34*, 285−290.
(63) Heredia, K. L.; Maynard, H. D. *Org. Biomol. Chem.* **2007**, *5*, 45−53.
(64) Gauthier, M. A.; Klok, H.-A. *Chem. Commun.* **2008**, 2591−2611.
(65) Qi, Y.; Chilkoti, A. *Polym. Chem.* **2014**, *5*, 266−276.
(66) Lee, S.; Greenwald, R. B.; McGuire, J.; Yang, K.; Shi, C. *Bioconjugate Chem.* **2001**, *12*, 163−169.
(67) Tucker, B. S.; Sumerlin, B. S. *Polym. Chem.* **2014**, *5*, 1566−1572.

DOI: 10.1021/acs.biomac.5b00623
Biomacromolecules XXXX, XXX, XXX−XXX